

Article

Nanosized Silica-Supported 12-Tungstophosphoric Acid: A Highly Active and Stable Catalyst for the Alkylation of *p*-Cresol with *tert*-Butanol

Walaa Alharbi ^{1,*}, Khadijah H. Alharbi ¹, L. Selva Roselin ¹, R. Savidha ² and Rosilda Selvin ³

¹ Department of Chemistry, Science and Arts College, King Abdulaziz University, Rabigh 21911, Saudi Arabia; slous@kau.edu.sa (L.S.R.)

² Department of Chemistry, Providence College for Women, Spring Field, Bandishola, Coonoor 643104, India; savidharam@gmail.com

³ Department of Basic Sciences and Humanities, Don Bosco Institute of Technology, Kurla (W), Mumbai 400070, India

* Correspondence: wnhalharbe@kau.edu.sa

Abstract: 12-Tungstophosphoric acid supported on nanosilica (TPA/SiO₂) was employed as a catalyst for the tertiary butylation of *p*-cresol using tertiary butanol as an alkylating agent. The TPA/SiO₂ catalyst was synthesized using the wet impregnation method followed by steaming at 150 °C for 6 h. The catalysts were characterized by means of X-ray diffraction (XRD) and Transmission Electron Microscopy (TEM) analysis. The surface acidity of the untreated and steamed catalysts was characterized via FTIR and DSC thermal analysis using pyridine as a probe molecule. The fresh and spent catalysts were characterized via TGA analysis. The catalytic activity studies showed that the steamed catalyst displayed higher activity, with a higher desired yield of 2-*tert*-butyl cresol (2-TBC) compared to the untreated catalyst, and that this activity was related to the presence of stronger Brønsted acid sites in the steamed catalyst. A detailed analysis of the TPA/SiO₂ steamed catalyst was performed to study the effects of reactant time-on-stream, reactant feed rate, reaction temperature, and the molar ratio of *tert*-butanol to *p*-cresol. The optimum reaction temperature, *tert*-butanol/*p*-cresol molar ratio, feed rate, and time-on-stream were 413 K, a molar ratio of 2:1, 6 mL/min, and 2 h, respectively. The present study demonstrates that the TPA/SiO₂ catalyst exhibits high activity in terms of % conversion and high % selectivity of 2-TBC under the optimized conditions. The characterization of fresh and spent catalysts confirmed the occurrence of coke deposition after the catalytic reaction. The catalyst was regenerated via heat treatment at 400 °C for 5 h. The regenerated catalyst was reused for subsequent runs for three cycles without showing a loss in its activity.

Keywords: *p*-cresol; *tert*-butanol; heteropoly acid; alkylation; TPA/SiO₂ catalyst; 2-*tert*-butyl-*p*-cresol; 2,6-di-*tert*-butyl-*p*-cresol; Brønsted and Lewis acid sites



Citation: Alharbi, W.; Alharbi, K.H.; Roselin, L.S.; Savidha, R.; Selvin, R. Nanosized Silica-Supported 12-Tungstophosphoric Acid: A Highly Active and Stable Catalyst for the Alkylation of *p*-Cresol with *tert*-Butanol. *Catalysts* **2023**, *13*, 1432. <https://doi.org/10.3390/catal13111432>

Academic Editor: Ioannis D. Kostas

Received: 7 October 2023

Revised: 27 October 2023

Accepted: 30 October 2023

Published: 13 November 2023



Copyright: © 2023 by the authors. Licensee MDPI, Basel, Switzerland. This article is an open access article distributed under the terms and conditions of the Creative Commons Attribution (CC BY) license (<https://creativecommons.org/licenses/by/4.0/>).

1. Introduction

The butylation of cresol is an industrially important reaction because it leads to the formation of corresponding value-added products like *o*-*tert*-butyl-*p*-cresol and *o*-di-*tert*-butyl-*p*-cresol, which are commercially known as butylated hydroxytoluene (BHT). These BHTs are widely used in the production of varnish and phenolic resins serving as antioxidants in food industries, polymerization inhibitors, and light protectors [1–4]. The derivatives of alkyl cresols are used as herbicides, bactericides, insecticides, etc. [5,6]. Alkylated cresols with an alkyl group including 9–12 carbon atoms are valuable intermediates for surfactants and nonionic detergents [7,8].

Techniques enabling the selective alkylation and acylation of aromatic substrates with an appropriate catalyst and yielding a desired product are in demand. The conventional Friedel–Crafts catalysts, such as AlCl₃, FeCl₃, and ZnCl₂, are least preferred as alkylating

agents owing to problems related to safety, handling, the requirement for stoichiometric quantities, the presence of several undesirable side products, the non-recycling of catalysts, waste disposal, and corrosion. To avoid these problems, much attention has been paid to environmentally friendly solid acid catalysts [9–11]. Solid acid catalysts supported on transition metal oxides in electrophilic aromatic substitutions with greater selectivity and safety are developed as substitutes for Lewis or mineral acids [12,13]. The use of ion-exchange resin plays a key role in the corresponding alkylation [14]. Cation exchange resin and modified sulfonic acid resin were used for the butylation of *p*-cresol [15]. Santacesaria et al. studied the kinetics of the alkylation of *p*-cresol with isobutene catalyzed by cation exchange resins, particularly Amberlyst-15 [16]. Though these catalysts are environmentally friendly, they cannot be used at elevated temperatures and have low activity [17,18].

Butylation was studied over sulfated zirconia and zirconia-supported heteropoly acids [15,19]. Yadav et al. reported a detailed study on the kinetics of the alkylation of *p*-cresol with isobutylene over a sulfated zirconia catalyst [20]. Based on the reaction temperature and acidity, C-alkylated and O-alkylated products were formed [21,22]. Though sulfated zirconia is a highly active solid catalyst due to its superior acidity, its applications are limited due to its poor stability, tendency to form volatile sulfur compounds during the reaction, and limited surface-active sites [23–25]. It was later designed in such a way that the super acidic characteristic of zirconia and sulfated zirconia was combined with a support material that possesses high surface area and high thermal stability. Various support materials, such as silica [26,27], MCM-41 [28], SBA-15 [29], zeolites [30], and Al₂O₃ [31], were tested for this alkylation. Sarish et al. studied the alkylation of *p*-cresol with *tert*-butanol over WO_x/ZrO₂ catalysts and the corresponding catalytic activity, which was compared with sulfated zirconia and zeolites like USY, H, and montmorillonite K-10, under optimized reaction conditions and concluded that the activity of sulfated zirconia was lower than that of the WO₃/ZrO₂ catalyst [32]. Malpani et al. designed a perlite-supported sulfated zirconia catalyst for the alkylation of isomeric cresols with *tert*-butyl alcohol, and the study revealed better conversion with few limitations [33].

Extensive research was carried out on the tertiary butylation of organic compounds over zeolites [34–37], but the application of zeolite is limited in the alkylation of bulky reactant molecules due to the mass transfer limitations experienced by microporous solids. Various alkylating agents have been studied on a few catalysts, such as SiO₂–Al₂O₃, γ -alumina, and zeolites, but their catalytic performance was limited by diffusional constraints related to different types of pores [22]. Mesoporous Al-MCM-41 is the better alternative in terms of rectifying the limitations exhibited by microporous materials [38,39] that have unique properties like highly-ordered mesopores, large surface area, high thermal stability, and mild acidity, which enhance the catalytic activity of mesoporous Al-MCM-41 in the alkylation of large molecules. Mesoporous solid acid catalysts are active with regard to and selective for the alkylation of aromatics [40–42]. The selective liquid-phase *t*-butylation of *p*-cresol with *t*-butyl alcohol (*t*-BuOH) to produce 2-*t*-butyl-*p*-cresol (TBC) over Al-MCM-41 catalysts was performed by Selvaraj et al., and the optimum conditions were reported for better selectivity [43]. Kamalakar et al. studied the *t*-butylation of *p*-cresol under a supercritical CO₂ atmosphere to minimize the use of organic solvents for environmentally conscious chemical processes, and the study emphasized that tungsten phosphoric acid/MCM-41 and H-Y zeolites exhibited better catalytic performance for the *t*-butylation of *p*-cresol [44].

Heteropolyacids and their salts (HPA) have drawn much attention due to their strong acidic character, oxidation ability, and unique “pseudo-liquid behavior [45]. Heteropoly acids supported on solid metal oxides have been gaining importance as alkylating and acylating catalysts [46–48]. Keggin type HPA and 12-tungstophosphoric acid (TPA) have been widely studied because of their stability [49,50]. Supported heteropoly anions on Al₂O₃ [51], SiO₂ [52], and MCM-41 molecular sieves [53] have been reported. TPA supported on different supports is used for the alkylation of various substrates. Su and Wang reported the *t*-butylation of *p*-cresol catalyzed by TPA immobilized on macroporous phenol-furfural sulfonic acid resin using a γ -aminopropyltriethoxy silane catalyst, and the results

revealed that the catalyst maintained the desired product selectivity and exhibited high activity for the *t*-butylation of *p*-cresol with *t*-butanol [15]. Devassy et al. reported the performance of a TPA/ZrO₂ catalyst in the butylation of *p*-cresol with *tert*-butanol; the catalyst was found to be highly active and stable and could be used efficiently in the alkylation reactions [19,54]. Bhatt et al. reported the *tert*-butylation of cresols using TPA and TPA supported on neutral alumina catalysts, and the results showed high conversion and high selectivity of the desired products [55]. The catalytic activity of Titania-supported TPA was evaluated for the alkylation of *p*-cresol with *tert*-butanol, and the results were compared with those for sulfated zirconia, zeolites like USY, H-, and montmorillonite K-10 catalysts under optimized identical reaction conditions. The heteropoly-acid-modified titania catalysts showed higher activity than the sulfated zirconia catalyst [56]. In the present study, silica (SiO₂) nanoparticles are used as a support. Silica nanoparticles contain many surface hydroxyl groups and are therefore hydrophilic in nature. This causes them to attract the hydrophilic TPA particles on the surfaces of silica nanoparticles, and, eventually, strong adhesion makes them a true heterogeneous catalyst.

The present study aims to report the performance of a TPA/SiO₂ catalyst in relation to the butylation of *p*-cresol with *tert*-butanol. Different reaction parameters, such as reaction temperature, reactant feed rate, the time of the reaction, and the molar ratio of the reactants, were systematically investigated and optimized.

2. Results and Discussion

2.1. XRD Analysis

The XRD powder diffraction patterns of the TPA/SiO₂ samples with various loadings of TPA are shown in Figure 1. The patterns show that the primary peaks are related to silica support, and these results are in agreement with a previous report on the structure of SiO₂ [57]. The homogenous dispersion of TPA into the pores of silica was observed for the TPA/SiO₂ catalyst with a low loading (up to 25%) (Figure 1 (a) and (b)), and these results are in agreement with a previous study on 12-tungstophosphoric acid catalysts used for the liquid-phase dehydration of D-xylose [58]. In the case of a high TPA loading (more than 25%), the peaks related to TPA are visible (Figure 1 (c) and (d)). The scattering effect due to the presence of nanoscale particles is shown as a broad peak located at a 2θ range of 3–8°.

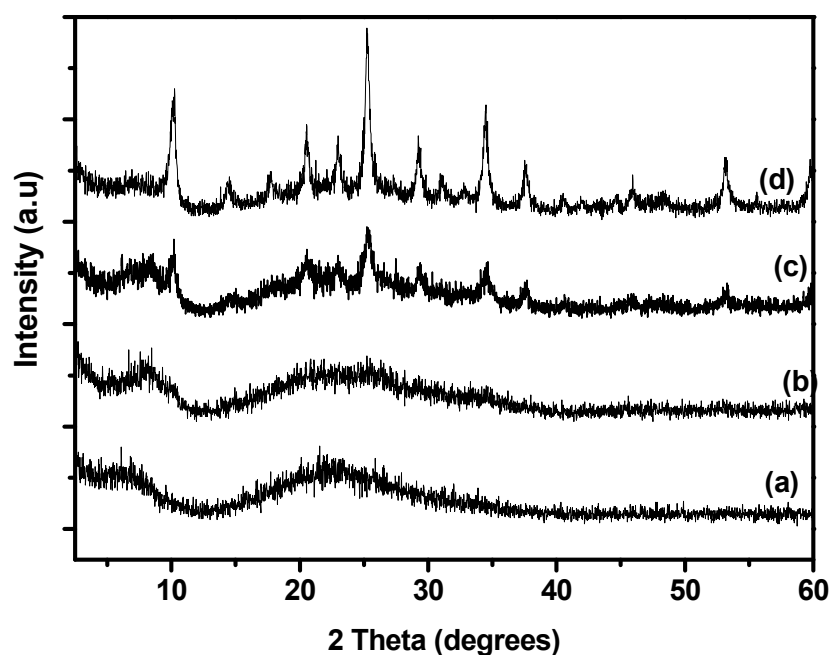


Figure 1. XRD patterns of TPA/SiO₂ with varying loadings of TPA: (a) 20 wt%; (b) 25 wt%; (c) 30 wt%; (d) 35 wt%.

The XRD pattern of the TPA/SiO₂ (25%) sample before and after steaming is presented in Figure 2. No peak for TPA was observed in TPA/SiO₂ samples before and after steaming, demonstrating the absence of free TPA particles on the surface of silica. This result confirms that the TPA particles are present inside the pores of the silica particles.

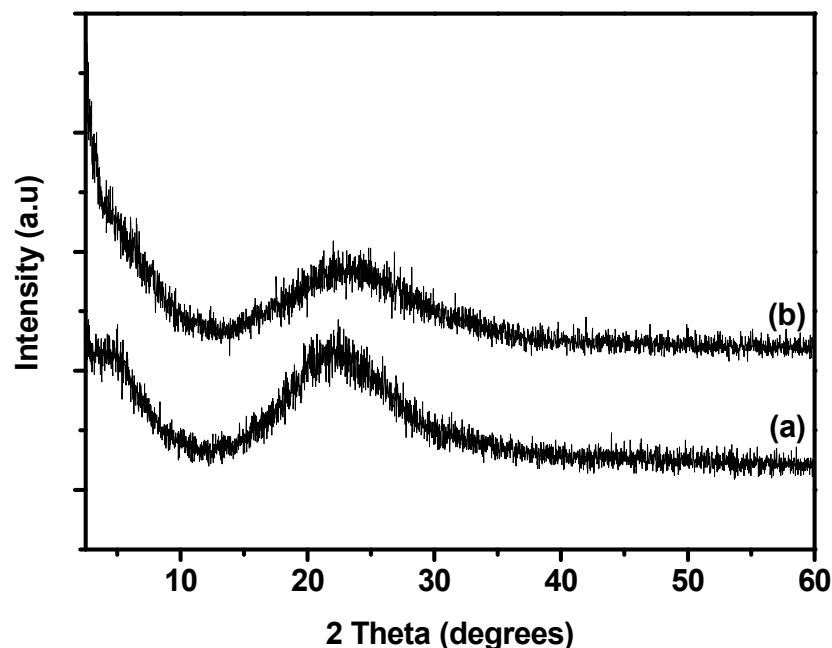


Figure 2. XRD patterns of TPA/SiO₂: (a) before steaming; (b) after steaming.

2.2. TEM Analysis

The TEM micrographs of the TPA/SiO₂ samples before and after steaming are presented in Figure 3. The TEM image of the TPA/SiO₂ sample before steaming shows that the particles are aggregated, as seen in Figure 3a; hence, the particle size could not be measured. The TPA/SiO₂ sample after steaming shows a homogeneous dispersion of the particles with an average crystal size of about 5 nm, as shown in the TEM image (Figure 3b). The homogeneous distribution of particles in the TPA/SiO₂ sample after steaming was attributed to the dissolution of TPA and silica particles followed by the recrystallisation of TPA on the silica nanoparticles [59]. As a result of the steaming process, the catalyst contained much more uniform crystals.

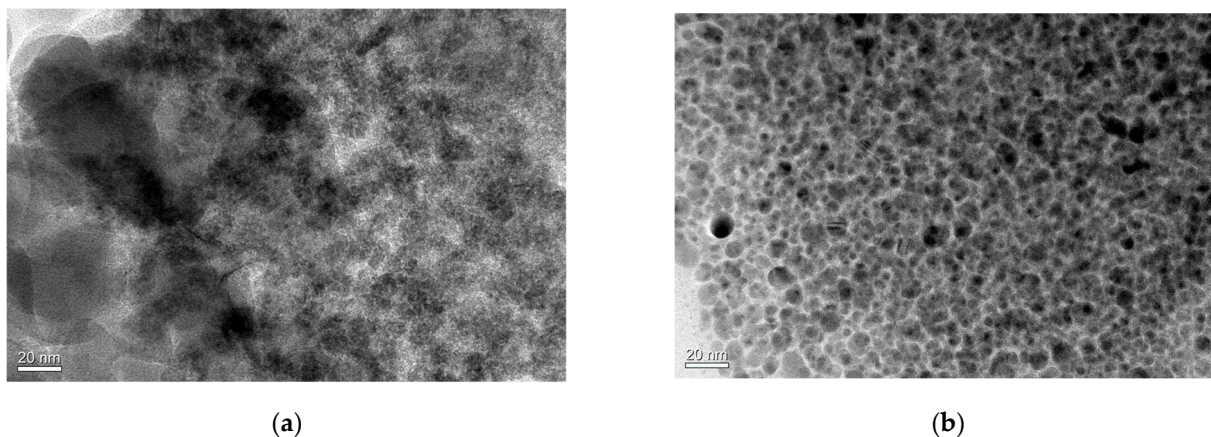


Figure 3. TEM images of TPA/SiO₂: (a) before steaming; (b) after steaming.

2.3. Surface Acidity of the TPA/SiO₂ Catalysts

The alkylation of *p*-cresol with *tert*-butanol was influenced by the nature, density, and strength of the acidic sites of the catalyst [54]. Hence, in the present study, the nature of the acidic sites was analyzed using pyridine-adsorbed IR and DSC techniques, in which pyridine was used as a probe molecule. Lewis and Brønsted acid sites were differentiated using the ring vibration modes [19]. Pyridine can interact with Brønsted acid sites to form pyridinium ions and with Lewis acid sites to form a coordination complex. The vapor-phase adsorption of pyridine over the TPA/SiO₂ (25%) sample before and after steaming was carried out according to a procedure described in the literature [60]. FTIR spectral data of the pyridine-adsorbed catalyst samples were studied to reveal the nature of the acid sites. The strength of the acid sites was analyzed using differential scanning calorimetric studies applied to the pyridine-adsorbed catalyst samples. The pyridine-adsorbed catalyst samples, TPA/SiO₂ (25%), before and after steaming, were subjected to a temperature scan between 30 and 550 °C at a heating rate of 10 °C min⁻¹. A nullifying technique was used, employing the sample cell and a reference cell containing 20 mg of the pyridine-adsorbed catalyst sample and the corresponding pyridine-free sample, respectively, at atmospheric pressure with nitrogen as a carrier gas [61].

Figure 4 depicts the DSC curves of pyridine desorption from the as-synthesized TPA/SiO₂ and steam-treated TPA/SiO₂ catalyst samples, and the results are shown in Table 1. The enhancement in the strength of Lewis acid sites (LA) and Brønsted acid sites (BA) is noted for the steamed samples of TPA/SiO₂ (25%) in comparison with the weak Lewis acid sites and Brønsted acid sites observed in the silica-nanoparticle-supported heteropoly acid TPA/SiO₂ (25%). This enhancement could have been due to the increased heat of desorption of pyridine from 632 to 1356 J/g and 286 to 445 J/g for the Lewis acid sites and Brønsted acid sites respectively (Figure 4).

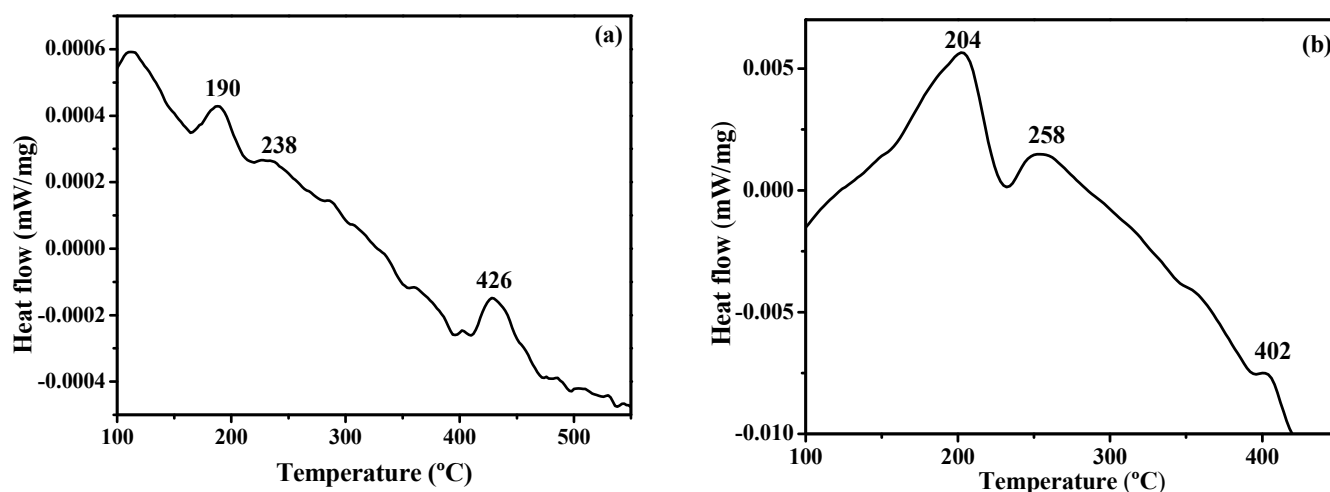


Figure 4. DSC curves for pyridine adsorption of TPA/SiO₂ (25%) (a) without steaming and (b) after steaming.

Table 1. DSC peak after pyridine adsorption of 12-tungstophosphoric acid.

| Name of Sample | Peak Temperature (°C) | ΔH (J/g) | Type of Acid Site |
|--|-----------------------|----------|-------------------|
| TPA/SiO ₂ 25% | 190 | 632 | LA ^a |
| | 426 | 286 | BA ^b |
| TPA/SiO ₂ 25% (After Steaming) | 204, 258 | 1356 | LA ^a |
| | 402 | 445 | BA ^b |

^a LA-pyridine desorption from Lewis acid sites; ^b BA-Pyridine desorption from Brønsted acid sites.

Figure 5A presents the FT-IR spectra of the TPA/SiO₂ sample and pyridine-adsorbed TPA/SiO₂ sample. The TPA/SiO₂ after steam treatment and the pyridine-adsorbed steam treated TPA/SiO₂ catalyst samples are shown in Figure 5B. The broad peak appearing at 1640 cm⁻¹ in all the samples before and after pyridine desorption is associated with weakly hydrogen-bonded water [62]. The noted increase in the intensity of the peak for both the pyridine-adsorbed samples is accounted for by the pyridinium ion formed via the interaction with Brønsted acid sites [63]. The appearance of peaks at 1540 cm⁻¹ and 1450 cm⁻¹ upon pyridine adsorption on the TPA/SiO₂ catalyst without steaming is shown in Figure 5A, whereas Figure 5B shows three peaks at 1540 cm⁻¹, 1490 cm⁻¹, and 1450 cm⁻¹ in the case of the pyridine-adsorbed TPA/SiO₂ sample after steaming. The coordinative adsorption of pyridine on Lewis acid sites indicated by the peak at around 1490 cm⁻¹ is due to overlapping vibrations. The peak at 1450 cm⁻¹ is characteristic of the adsorption of pyridine on both Lewis and Brønsted acid sites [64]. Higher densities of Lewis acid sites (1450 cm⁻¹) and Brønsted acid sites (1540 cm⁻¹, 1490 cm⁻¹, and 1640 cm⁻¹) were observed in the TPA/SiO₂ catalyst sample after steaming compared to the as-synthesized sample without steaming.

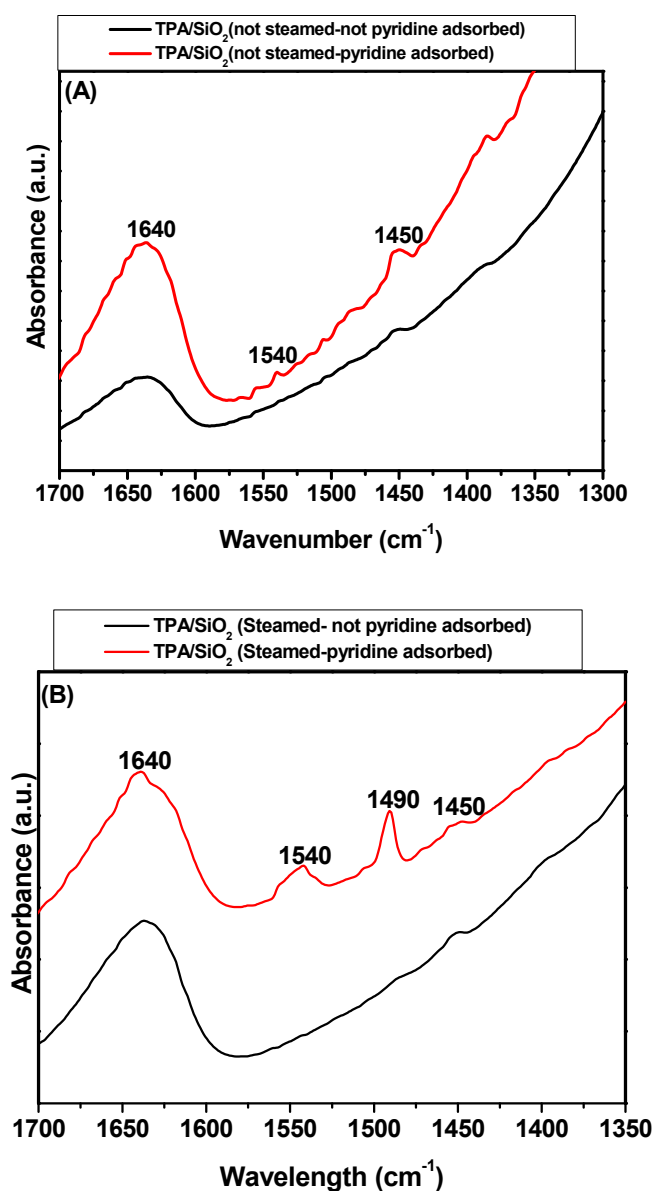


Figure 5. FTIR spectra for TPA/SiO₂ (25%) samples before and after pyridine adsorption: (A) without steaming; (B) after steaming.

2.4. Thermogravimetric Analysis (TGA) of Fresh and Used Catalyst

The TGA profiles for both the fresh and used catalysts are shown in Figure 6. It can be seen that at temperatures below 200 °C, weight loss of approximately 7% and 12% was observed in the TG thermogram for both the fresh and used catalysts, respectively, which could have been due to the loss of loosely bonded water. From 200 to 400 °C, weight loss values of approximately 2% and 3% for the fresh and used catalysts were recorded, and this weight loss is associated with the strongly bonded water [65]. In the case of the fresh catalyst, further weight loss was not observed. The weight loss that occurred for the used catalyst between 350 and 800 °C might have resulted from the decomposition of coke formed during the reaction [66]. The burning off of the deposited “hard” carbon species [67] at high temperatures could be the reason for this loss, and this process accounts for the blockage of the active center and the catalyst’s deactivation at high time-on-stream. The accumulation of organic compounds on a catalyst during this reaction was observed in previous studies [68].

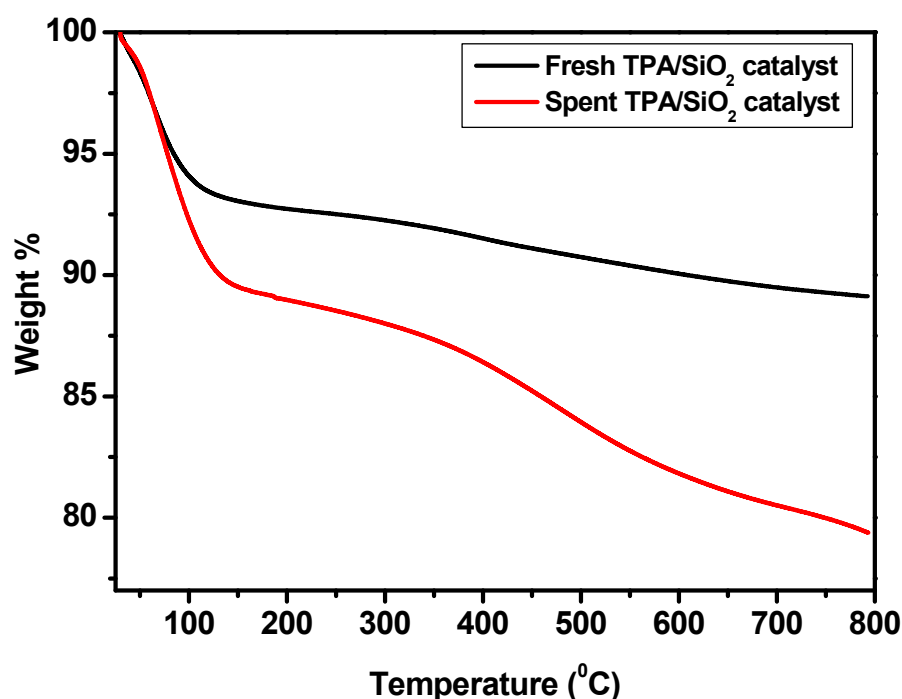
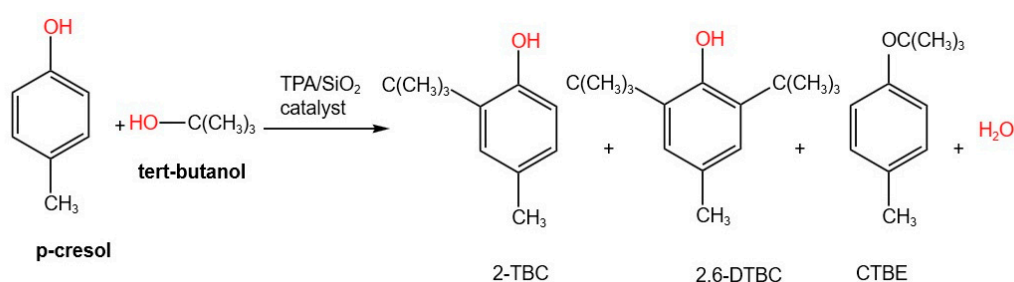


Figure 6. Thermogravimetric analysis (TGA) of the fresh and spent TPA/SiO₂ catalysts.

2.5. Catalytic Studies

The tertiary butylation of *p*-cresol with *t*-BuOH catalyzed by 12-tungstophosphoric acid impregnated on nano silica (25% TPA/SiO₂) is an electrophilic substitution reaction occurring on the aromatic ring. This reaction proceeds through both C-alkylation and O-alkylation. The C-alkylated products obtained are 2-*tert*-butyl cresol (2-TBC) and 2,6-di-*tert*-butyl cresol (2,6-DTBC). The o-alkylated product obtained is cresol-*tert*-butyl ether (CTBE). The 2-TBC was obtained as a major product, and 2,6-DTBC and CTBE were obtained in small quantities. The reaction scheme is shown in Scheme 1. A similar product distribution was reported in previous studies on copper-based nanocatalysts [69]. To achieve the maximum conversion and selectivity of the desired product, the reaction parameters such as reaction temperature, reactant feed rate, time-on-stream, and the molar ratio of *tert*-butanol to *p*-cresol were optimized.



Scheme 1. Tertiarybutylation of *p*-cresol with *t*-BuOH catalyzed by 12-tungstophosphoric acid supported on nanosilica (TPA/SiO₂).

2.5.1. Effect of Steam Treatment

Table 1 compares the as-synthesized TPA/SiO₂ and the steam-treated TPA/SiO₂ in terms of their performance in the *tert*-Butylation of *p*-cresol. These catalysts were used to study the effect of steam treatment on the catalytic efficiency of the *tert*-Butylation of *p*-cresol. The experiments were carried out under an identical set of conditions. A 0.15 g loading of catalyst was taken, and the reaction temperature was maintained at 413 K, the feed rate was maintained at 6 mL/h, and a molar ratio of *tert*-butanol to *p*-cresol of 2:1 was ensured. It was found that the steam-treated catalyst exhibited higher conversion compared to the untreated catalyst (Table 2).

Table 2. Catalytic activity of steamed and non-steamed TPA/SiO₂ catalyst on tertiary butylation of *p*-cresol with *t*-BuOH.

| Catalyst | Conversion (wt.%) | | | |
|------------------------|-------------------|-------|---------|------|
| | <i>p</i> -Cresol | 2-TBC | 2,6-TBC | CTBE |
| Untreated catalyst | 61.8 | 85.7 | 3.8 | 10.5 |
| Steam-treated catalyst | 92 | 90.4 | 8.5 | 1.1 |

The higher activity of the steamed TPA/SiO₂ catalyst was due to the enhanced strength of the Brønsted acid sites after steaming (Figures 4 and 5 and Table 1). The increase in acid sites enhances the diffusion of the reactants and improves the catalytic activity, as evident from a previous report [70].

2.5.2. Effect of Time-on-Stream

The activity of the 25% TPA/SiO₂ catalyst was investigated as a function of time in the butylation of *p*-cresol at 413 K and a feed rate 6 mL/h and with a *tert*-butanol-to-*p*-cresol molar ratio of 2:1. This study was conducted for 12 h, the products were collected and analyzed each hour, and the results are presented in Figure 7. When the reaction time increased from 1 h to 6 h, a gradual decrease in the conversion of *p*-cresol from 93.6 to 76.7% was observed (Figure 7A). The selectivity of 2-TBC increased to 4 h and then attained a steady state (Figure 7B). The formation of ether (CTBE) was negligible; this reveals the stability of the catalyst in the presence of polar reactants, which attracts much attention for industrially important reactions [19]. The gradual decrease in conversion with time-on-stream after 2 h was due to the deactivation of the catalyst caused by coke deposition on the active sites, as evident from the TGA analysis of the spent catalyst (Figure 6). Chen et al. [71] detected the blockage of active sites by coke formed during the reaction, which causes a deterioration in catalytic activity. Considering the above observations, 2 h was chosen as a suitable time-on-stream for further study.

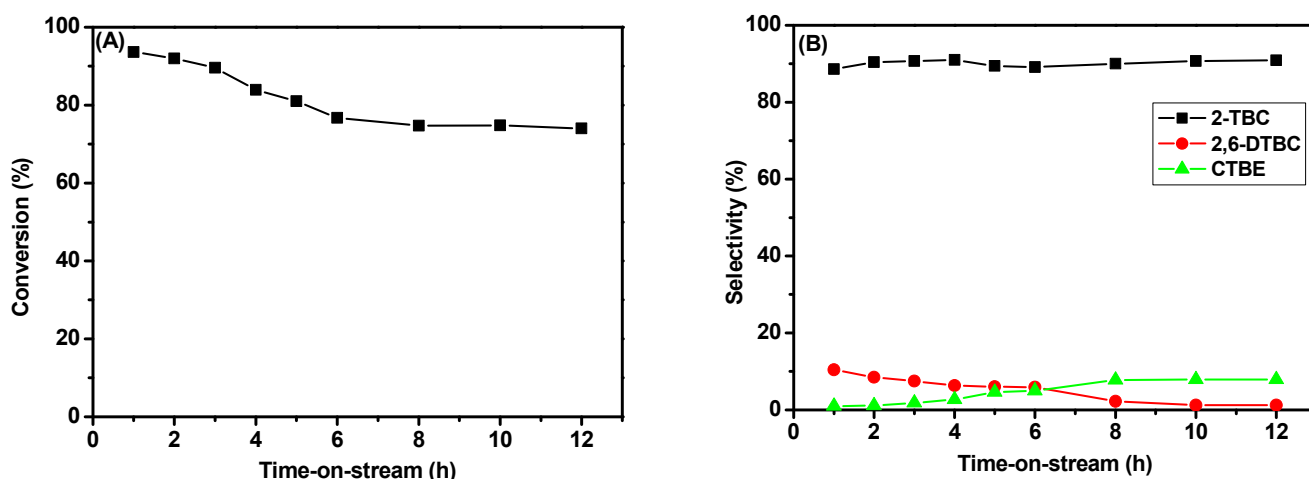


Figure 7. Effect of time-on-stream on the catalytic activity of 25%TPA/SiO₂ catalyst for the tertiary butylation of *p*-cresol with *t*-BuOH. (A) Conversion vs. TOS; (B) selectivity vs. TOS.

Reaction conditions: TPA/SiO₂ catalyst weight: 1 g; *tert*-butanol-to-*p*-cresol molar ratio: 2; feed rate: 6 mLh⁻¹; reaction temperature: 413 K.

2.5.3. Effect of Reactant Feed Rate

The *Tert*-butylation of *p*-cresol on TPA/SiO₂ was carried out at different feed rates ranging from 6 to 12 mL/h at 413 K with a butanol/*p*-cresol molar ratio of 2, and the results are shown in Figure 8.

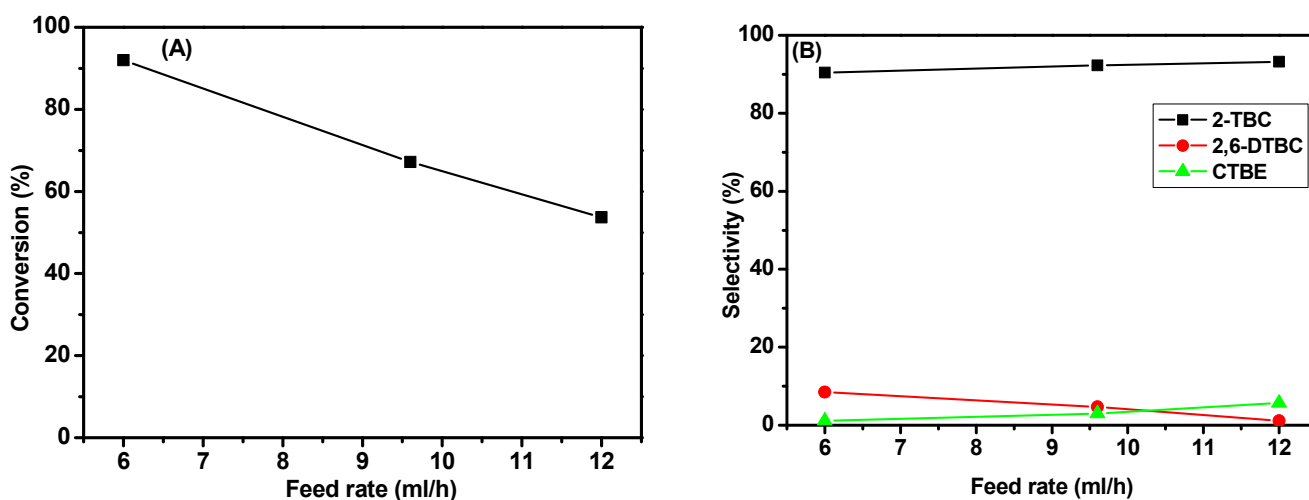


Figure 8. Effect of feed rate on the catalytic activity of 25% TPA/SiO₂ catalyst on the tertiary butylation of *p*-cresol with *t*-BuOH. (A) Conversion versus feed rate; (B) selectivity versus feed rate.

Reaction conditions: TPA/SiO₂ catalyst weight: 1 g; *tert*-butanol-to-*p*-cresol molar ratio: 2; time-on-stream: 2 h; reaction temperature: 413 K.

At a feed rate of 6 mL/h, a maximum conversion of about 92% of *p*-cresol was obtained along with the majority of the C-alkylated product and a selectivity of 2-TBC of 90.4%. The selectivity of 2-TBC remained almost unchanged for all the feed rates studied. With an increasing feed rate, the % conversion of *p*-cresol decreased due to the shorter contact time (Figure 8A). However, the selectivity of 2,6-DTBC was found to be greater at lower feed rates and decreased with an increase in feed rate (Figure 8B). Longer contact time favored 2,6-DTBC formation (8.5%), while less contact time enabled ether formation (5.7%), and the water formed in this reaction hinders the alkylation of cresol [53]. Considering the %

conversion of *p*-cresol and the % selectivity of the products, the optimum feed rate was fixed at 6 mL/min.

2.5.4. Effect of Reaction Temperature

The effect of reaction temperature on the catalytic activity of the TPA/SiO₂ catalyst for the tertiary butylation of *p*-cresol was studied at different temperatures ranging from 393 K to 453 K at a constant feed rate of 6 mLh⁻¹ with a *tert*-butanol-to-*p*-cresol molar ratio of 2, and the results are presented in Figure 9. At 373K, the conversion of *p*-cresol was 75.5%, and it increased to 92% at 413 K. The selectivity toward 2-TBC and 2,6-DTBC was increased with an increasing temperature. On the other hand, the selectivity toward ether (CTBE) decreased with an increasing temperature. The lower temperature favored CTBE formation, and it decreased at higher temperatures; this finding was attributed to the dealkylation of the alkylated products and the reduced availability of *tert*-butanol due to the fact that oligomerization rather than alkylation occurred [72]. The highest conversion of *p*-cresol and level of 2-TBC selectivity were observed at 413 K (Figure 6). Based on the observation of the conversion of *p*-cresol and the selectivity towards 2-TBC formation, the optimum reaction temperature was fixed at 413 K.

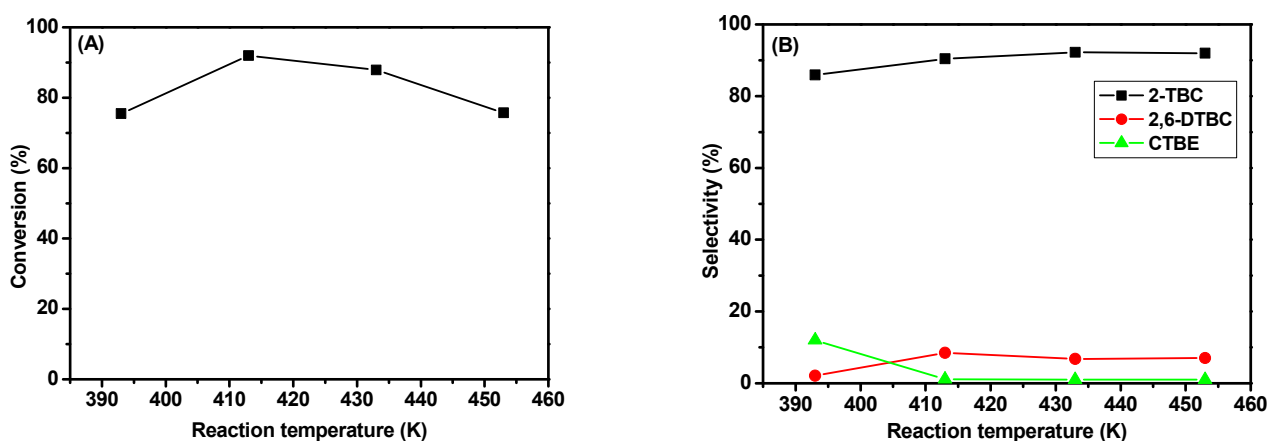


Figure 9. Effect of reaction temperature on the catalytic activity of 25%TPA/SiO₂ catalyst toward the tertiary butylation of *p*-cresol with *t*-BuOH. (A) Conversion vs. reaction temperature; (B) selectivity vs. reaction temperature.

Reaction conditions: TPA/SiO₂ catalyst weight: 1 g; *tert*-butanol-to-*p*-cresol molar ratio: 2; feed rate: 6 mLh⁻¹; time-on-stream: 2 h.

2.5.5. Effect of Molar Ratio of *tert*-Butyl Alcohol to *p*-Cresols

The correlation between the molar ratio of *tert*-butyl alcohol/*p*-cresols with respect to the conversion of *p*-cresols and the selectivity of the products was studied by carrying out reactions at varying molar ratios ranging from 1 to 4 over the TPA/SiO₂ catalyst at 413 K. A remarkable increase in the conversion of *p*-cresol was noticed after increasing the molar ratio from 1 to 2 and then allowing the reaction to reach a steady state, as shown in Figure 10A.

Reaction conditions: TPA/SiO₂ catalyst weight: 1 g; feed rate: 6 mLh⁻¹; reaction temperature: 413 K; time-on-stream: 2 h.

The lower conversion of *p*-cresol at a lower molar ratio of *tert*-butanol to *p*-cresol could be due to the preferential adsorption of *p*-cresol over *tert*-butanol on the catalyst's surface owing to its polar character. When increasing the molar ratio of *tert*-butanol to *p*-cresol, conversion increased, which could be attributed to the higher concentration of tertiary butanol [55]. Among the molar ratios studied, the products obtained were 2-TBC, 2,6-DTBC, and CTBE, with 2-TBC being the major product (Figure 10B). The % selectivity of 2-TBC increased when the molar ratio increased from 1 to 2, and this increase became negligible

afterwards. The % selectivity of 2,6-DTBC increased when increasing the concentration of *tert*-butyl alcohol due to the greater resident time of the mono *tert*-butylated product on the catalyst surface [33]. As the conversion of *p*-cresol and the selectivity toward 2-TBC are higher at a molar ratio of *p*-cresol to tertiary butanol of 1:2, the optimum molar ratio was fixed at 1:2.

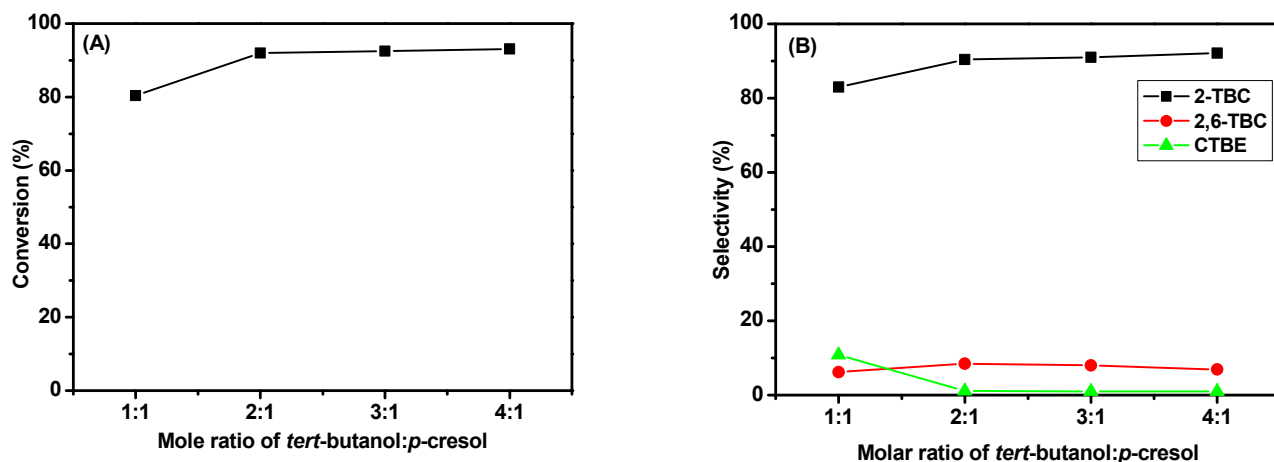


Figure 10. Effect of molar ratio of *tert*-butyl alcohol/cresols on the catalytic activity of 25% TPA/SiO₂ catalyst toward the tertiary butylation of *p*-cresol with *t*-BuOH. (A) Conversion vs. molar ratio of *tert*-butanol/*p*-cresol; (B) selectivity vs. molar ratio of *tert*-butanol/*p*-cresol.

2.5.6. Reusability of the Catalyst

In heterogeneous catalytic reactions induced using a fixed bed reactor under vapor-phase condition, it is important to reuse the catalyst so that it may be commercialized in the chemical industry. The TPA/SiO₂ catalyst was reused for subsequent runs for the *tert*-butylation of *p*-cresol after regeneration via heating at 400 °C for 5 h. Figure 11 shows the reusability test results for the *t*-Butylation of *p*-cresol at 413 K for a 2:1 molar ratio of *t*-butanol/*p*-cresol. The reusability test demonstrated that the catalyst could maintain good catalytic performance in the alkylation of *p*-cresol with tertiary butanol repeatedly for three subsequent runs as it exhibited a conversion of *p*-cresol and selectivity for 2-TBC in the range of 92% and 90%, respectively. No appreciable change in the catalytic activity of the catalyst was observed after it was used three times. The results demonstrate that the TPA/SiO₂ catalyst was recoverable and recyclable and can be repeatedly used in industrial applications.

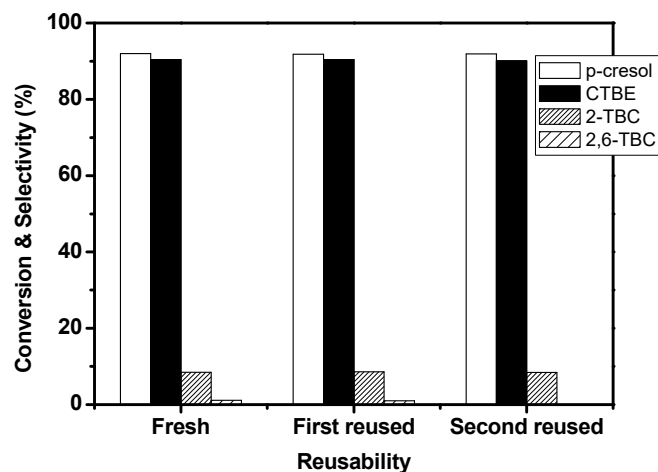


Figure 11. Reusability of 25% TPA/SiO₂ catalyst on the tertiary butylation of *p*-cresol with *t*-BuOH.

Reaction conditions: TPA/SiO₂ catalyst weight: 1 g; feed rate: 6 mLh⁻¹; reaction temperature: 413 K; time-on-stream: 2 h; *tert*-butanol-to-*p*-cresol molar ratio: 2:1.

3. Materials and Methods

3.1. Chemicals

Tetraethoxysilane (TEOS), *p*-cresol, *tert*-butanol, and 12-Tungstophosphoric acid were purchased from Merck and used as received.

3.2. Preparation of 12-Tungstophosphoric Acid Supported on Silica Catalysts

12-Tungstophosphoric acid supported on silica (TPA/SiO₂) catalyst was prepared using the sol-gel method followed by steaming. A series of catalysts with different TPA loadings (20–35%) were prepared by varying the TPA concentration over the silica support. As in a typical procedure for preparing 25% TPA/SiO₂, 12-Tungstophosphoric acid (2.5 g) was dissolved in deionized water (10 mL). Tetraethoxysilane was mixed with ethanol (34.7 g of TEOS and 20 g of EtOH) and dropped into the above solution under vigorous stirring for 30 min. The transparent gel was subjected to vacuum evaporation at 60 °C, yielding sugar-like cubes. The solid was crushed and dried in an air oven at 120 °C for 6 h. The dried powder was steamed at 150 °C for 6 h (S-TPA/SiO₂).

3.3. Characterization Methods

Powder X-ray diffraction patterns were recorded using a Rigaku 2000 diffractometer (Tokyo, Japan) equipped with Cu-K α radiation ($\lambda = 1.5418 \text{ \AA}$) from $2\theta = 2.5$ to 60° at a scan rate of $2^\circ/\text{min}$ using a step size of 0.04° . The morphology and particle size examinations of the samples were carried out using TEM analysis (JEM-2010, 200kV) (Jeol Co., Tokyo, Japan). Surface acidity of the TPA/SiO₂ (25%) catalyst before and after steaming was characterized via differential scanning calorimetry (DSC) (DSC-60A, Shimadzu, Tokyo, Japan) and FTIR techniques after pyridine adsorption. DSC analysis was conducted using a DSC 60 instrument. FT-IR spectra were recorded using a JASCO-FT/IR-6800 spectrophotometer (Hachioji, Tokyo, Japan). The fresh and spent catalysts were characterized via Thermogravimetric (TGA) analysis with a Perkin-Elmer TGA-7 analyzer (Perkin Elmer, Shelton, CT, USA). The catalyst sample (30 mg) was loaded in the sample holder and heated under nitrogen atmosphere (flow rate of 30 mL/min) at a heating rate of $10^\circ\text{C}/\text{min}$ in the temperature range of 25°C to 800°C .

3.4. Catalytic Testing

Tert-Butylation of *p*-cresol using *tert*-butanol was carried out under vapor-phase conditions in a down flow fixed bed glass reactor (i.d. 15 mm and length 300 mm) at atmospheric pressure. About 1 g of the catalyst was loaded into the reactor, packed in a layer of ceramic wool, and supported by glass beads. The catalyst was activated at 450°C under air flow for 5 h. The reactor was heated to the reaction temperature with the help of a tubular furnace controlled via a digital temperature controller. *p*-Cresol and tertiary butanol in a desired molar ratio were fed into the reactor with a fixed feed rate (ml h^{-1}) using a syringe pump at the optimum reaction temperature. The products were collected at the bottom via circulating cold water and analyzed using a China gas chromatograph (8990) with a capillary column (SE-52) and a flame ionization detector (FID). The products were identified and confirmed using GC-MS (Varian star 3400 GC) (Varian, Inc., Walnut Creek, CA, USA).

4. Conclusions

The catalytic activity of 12-tungstophosphoric acid impregnated on nanosilica (TPA/SiO₂) was tested with regard to the alkylation of *p*-cresol with tertiary butanol in vapor-phase conditions. More than 90% conversion of *p*-cresol and 92% 2-TBC selectivity were achieved under the optimum reaction conditions, namely, a reaction temperature of 413 K, a feed rate of 6 mL/h, and a molar ratio of *tert*-butyl alcohol/cresol of 2:1. Investigations comparing

the catalytic activity and surface acidity of the as-synthesized TPA/SiO₂ catalyst and steamed TPA/SiO₂ catalyst confirmed that the enhanced Brønsted acid sites in the steamed catalyst helped to improve the catalytic activity for the alkylation of *p*-cresol with tertiary butanol. The catalyst can be recycled with no appreciable change in activity in terms of the conversion of *p*-cresol and the selectivity of the desired product (2-TBC). The silica support in TPA plays an important role in improving its activity compared to that of other supports (Zircinia and WO_x/ZrO₂), as reported in the literature [51]. The % conversions of *p*-cresol for TPA supported on Zircinia, WO_x/ZrO₂, and SiO₂ were 61%, 69.8%, and 90%, respectively. In addition, the TPA/SiO₂ could be reused without a decrease in activity, as no leaching was detected. A previous report on TPA immobilized on modified macroporous phenol-furfural sulfonic acid resin revealed that it underwent leaching, which resulted in a decrease in activity [15]. The present study reveals that the TPA/SiO₂ catalyst is highly efficient for the tertiary butylation of *p*-cresol with *tert*-butyl alcohol in order to produce 2-*tert*-Butyl cresol (TBC). Since the reaction was carried out in a fixed-bed reactor under vapor-phase conditions, with the resulting product presenting high activity and reusability, the TPA/SiO₂ catalyst is a suitable catalyst for industrial applications.

Author Contributions: W.A.: Investigation and Writing—original draft. K.H.A.: Investigation and Formal analysis. L.S.R.: Investigation, Methodology, and Formal analysis. R.S. (R. Savidha): Writing and review and editing. R.S. (Rosilda Selvin): Conceptualization, Methodology, and Formal analysis. All authors have read and agreed to the published version of the manuscript.

Funding: This research work was funded by Institutional Fund Projects under grant no. (IFPIP1443-665-1078). The authors gratefully acknowledge the technical and financial support provided by the Ministry of Education and King Abdulaziz University, DSR, Jeddah, Saudi Arabia.

Data Availability Statement: Data are contained within the article.

Conflicts of Interest: The authors declare that they have no known competing financial interest or personal relationship that could have appeared to influence the work reported in this paper.

References

1. Pospíšil, J. Mechanistic action of phenolic antioxidants in polymers—A review. *Polym. Degrad. Stab.* **1988**, *20*, 181–202. [[CrossRef](#)]
2. Huston, R.C.; Lewis, W.C. Action of aromatic alcohols on aromatic compounds in the presence of aluminum chloride. VII condensation of benzyl alcohol with para-cresol. *J. Am. Chem. Soc.* **1931**, *53*, 2379–2382. [[CrossRef](#)]
3. Murphy, J. *The Additives for Plastics Handbook*; Elsevier Advanced Technology: Oxford, UK, 1996.
4. Shinde, A.B.; Shrigadi, N.B.; Samant, S.D. *tert*-Butylation of phenols using *tert*-butyl alcohol in the presence of FeCl₃-modified montmorillonite K10. *Appl. Catal. A Gen.* **2004**, *276*, 5–8. [[CrossRef](#)]
5. Lebedev, N.N. Chemistry and Technology of Basic Organic and Petrochemical Synthesis. MIR Publishers. Moscow 1 and 2. *J. Polym. Sci. Part C Polym. Lett.* **1984**, *24*, 305. [[CrossRef](#)]
6. Melnikov, N.N.; Baskahov, Y.A.; Bokrev, K.S. Chemistry of herbicides and plant growth regulators. *Gkhi. Moscow* **1954**, *38–42*, 38–42.
7. Shreve, R.N.; Brink, J.A. *Chemical Process Industries*, 4th ed.; McGraw-Hill International Book Company: London, UK, 1977; pp. 812–814.
8. Dimitriev, S.A.; Korener, K.D.; Tsvetkov, O.N. Synthesis of detergents of *o,p*-type based on phenols derived from peat oils. *Torfyanyaya. Prom.* **1961**, *32*, 24–27.
9. Corma, A. Inorganic Solid Acids and Their Use in Acid-Catalysed Hydrocarbon Reactions. *Chem. Rev.* **1995**, *95*, 559–614. [[CrossRef](#)]
10. Clark, J.H.; Macquarrie, D.J. Environmentally friendly catalytic methods. *Chem. Soc. Rev.* **1996**, *25*, 303–310. [[CrossRef](#)]
11. Clark, J.H.; Macquarrie, D.J. Catalysis of liquid phase organic reactions using chemically modified mesoporous inorganic solids. *Chem. Commun.* **1998**, *8*, 853–860. [[CrossRef](#)]
12. Mizuno, N.; Misono, M. Heteropolyacid catalysts. *Curr. Opin. Solid State Mater. Sci.* **1997**, *2*, 84–89. [[CrossRef](#)]
13. Shubhashish, S.; Wijenayake, S.; Huang, X.; Posada, L.F.; Samantha Joy, B.R.; Khanna, H.S.; Dziengiel, D.; Mansour, A.; Suib, S.L. Highly Mesoporous MoO₃ Catalysts for Electrophilic Aromatic Substitution. *Appl. Mater. Interfaces* **2002**, *14*, 51041–51052. [[CrossRef](#)] [[PubMed](#)]
14. Hartmut, Die Alkylierung von *p*-Kresol mit Isobuten an polymeren Festsäuren. *Chem.-Ing.-Tech.* **1980**, *52*, 825. [[CrossRef](#)]
15. Su, Z.-R.; Wang, T.-J. 12-Tungstophosphoric acid immobilized on modified macroporous phenol-furfural sulfonic acid resin for *tert*-butylation of *p*-cresol. *React. Funct. Polym.* **1995**, *28*, 97–102. [[CrossRef](#)]

16. Santacessaria, E.; Silvani, R.; Wilkinson, P.; Carra, S. Alkylation of *p*-Cresol with Isobutene Catalysed by Cation-Exchange Resins: A Kinetic Study. *Ind. Eng. Chem. Res.* **1988**, *27*, 541–548. [[CrossRef](#)]
17. Harmer, M.A.; Sun, Q. Solid acid catalysis using ion-exchange resins. *Appl. Catal. A Gen.* **2001**, *221*, 45–62. [[CrossRef](#)]
18. Chandra, K.G.; Sharma, M.M. Alkylation of phenol with MTBE and other *tert*-butyl ethers: Cation exchange resins as catalysts. *Catal. Lett.* **1993**, *19*, 309–317. [[CrossRef](#)]
19. Devassy, B.M.; Shanbhag, G.V.; Lefebvre, F.; Halligudi, S.B. Alkylation of *p*-cresol with *tert*-butanol catalyzed by heteropoly acid supported on zirconia catalyst. *J. Mol. Catal. A Chem.* **2004**, *210*, 125–130. [[CrossRef](#)]
20. Yadav, G.D.; Thorat, T.S. Kinetics of Alkylation of *p*-Cresol with Isobutylene Catalyzed by Sulfated Zirconia. *Ind. Eng. Chem. Res.* **1996**, *35*, 721–731. [[CrossRef](#)]
21. DeCastro, C.; Sauvage, E.; Valkenberg, M.H.; Hölderich, W.F. Immobilised Ionic Liquids as Lewis Acid Catalysts for the Alkylation of Aromatic Compounds with Dodecene. *J. Catal.* **2000**, *196*, 86–94. [[CrossRef](#)]
22. Ono, Y. Role of Basic Sites in Catalysis by Zeolites. *Stud. Surf. Sci. Catal.* **1980**, *5*, 19–27.
23. Yadav, G.D.; Nair, J.J. Sulfated zirconia and its modified versions as promising catalysts for industrial processes. *Microporous Mesoporous Mater.* **1999**, *33*, 1–48. [[CrossRef](#)]
24. Sreenivasan, R.; Keogh, R.A.; Milburn, D.R.; Davis, B.H. Sulfated Zirconia Catalysts: Characterization by TGA/DTA Mass Spectrometry. *J. Catal.* **1995**, *153*, 123–130. [[CrossRef](#)]
25. Rahman, N.J.A.; Ramli, A.; Jumbri, K.; Uemura, Y. Tailoring the surface area and the acid–base properties of ZrO₂ for biodiesel production from *Nannochloropsis* sp. *Sci. Rep.* **2019**, *9*, 16223. [[CrossRef](#)]
26. Kuwahara, Y.; Kaburagi, W.; Fujitani, T. Catalytic conversion of levulinic acid and its esters to γ -valerolactone over silica-supported zirconia catalysts. *Bull. Chem. Soc. Jpn.* **2014**, *87*, 1252–1254. [[CrossRef](#)]
27. Ward, A.J.; Pujari, A.A.; Costanzo, L.; Masters, A.F.; Maschmeyer, T. Ionic liquid-templated preparation of mesoporous silica embedded with nanocrystalline sulfated zirconia. *Nanoscale Res. Lett.* **2011**, *6*, 192–199. [[CrossRef](#)] [[PubMed](#)]
28. Abdel Salam, M.S.; Betiha, M.A.; Shaban, S.A.; Elsabagh, A.M.; Abd El-Aal, R.M.; El Kady, F.Y. Synthesis and characterization of MCM-41-supported nano zirconia catalysts. *Egypt. J. Pet.* **2015**, *24*, 49–57. [[CrossRef](#)]
29. Tamizhdurai, P.; Sakthinathan, S.; Santhana Krishnan, P.; Ramesh, A.; Mangesh, V.L.; Abilarasu, A.; Narayanan, S.; Shanthi, K.; Chiu, T.W. Catalytic activity of ratio-dependent SBA-15 supported zirconia catalysts for highly selective oxidation of benzyl alcohol to benzaldehyde and environmental pollutant heavy metal ions detection. *J. Mol. Struct.* **2019**, *1176*, 650–661. [[CrossRef](#)]
30. Kim, K.D.; Kim, J.; Teoh, W.Y.; Kim, J.C.; Huang, J.; Ryoo, R. Cascade reaction engineering on zirconia-supported mesoporous MFI zeolites with tuneable Lewis–Brønsted acid sites: A case of the one-pot conversion of furfural to γ -valerolactone. *RSC Adv.* **2020**, *10*, 35318–35328. [[CrossRef](#)]
31. Bikmetova, L.I.; Kazantsev, K.V.; Zatulokina, E.V.; Dzhikiya, O.V.; Molikov, S.M.D.; Belyi, A.S. Sulfated zirconia catalysts supported on alumina for hexane isomerization. *AIP Conf. Proc.* **2020**, *2301*, 030002. [[CrossRef](#)]
32. Saris, S.; Devassy, B.M.; Halligudi, S.B. *tert*-Butylation of *p*-cresol over WO_x/ZrO₂ solid acid catalysts. *J. Mol. Catal. A Chem.* **2005**, *235*, 44–51. [[CrossRef](#)]
33. Malpani, S.K.; Goyal, D.; Chinnam, S.; Sharma, S.K.; Katara, S.; Rani, A. Vapor Phase Alkylation of Isomeric Cresols with *Tert*-Butyl Alcohol over Perlite Supported Sulfated Zirconia Catalyst. *Sustainability* **2000**, *14*, 5149–5170. [[CrossRef](#)]
34. Chumbhale, V.R.; Gore, K.U.; Hegde, S.G.; Kim, J.-S.; Lee, S.-B.; Choi, M.-J. Tertiary Butylation of Phenol over HY and Dealuminated HY Zeolites. *J. Ind. Eng. Chem.* **2003**, *9*, 748–752.
35. Dumitriu, E.; Hulea, V. Effects of channel structures and acid properties of large-pore zeolites in the liquid-phase *tert*-butylation of phenol. *J. Catal.* **2003**, *218*, 249–257. [[CrossRef](#)]
36. Anand, R.; Maheswari, R.; Gore, K.; Tope, B. Tertiary butylation of phenol over HY and dealuminated HY zeolites. *J. Mol. Catal. A Chem.* **2003**, *193*, 251–257. [[CrossRef](#)]
37. Padmasri, A.H.; Kumari, V.D.; Rao, P.K. Supported 12-tungstophosphoric acid: A recoverable solid acid catalyst for liquid phase Friedel–Crafts alkylation of phenol. *Stud. Surf. Sci. Catal.* **1998**, *113*, 561–563. [[CrossRef](#)]
38. Kresge, C.T.; Leonowicz, M.E.; Roth, W.J.; Vartuli, J.C.; Beck, J.S. Ordered mesoporous molecular sieves synthesized by a liquid-crystal template mechanism. *Nature* **1992**, *359*, 710–712. [[CrossRef](#)]
39. Beck, J.S.; Vartuli, J.C.; Roth, W.J.; Leonowicz, M.E.; Kresge, C.T.; Schmitt, K.D.; Chu, C.T.-W.; Olson, D.H.; Sheppard, E.W.; McCullen, S.B. A new family of mesoporous molecular sieves prepared with liquid crystal templates. *J. Am. Chem. Soc.* **1992**, *114*, 10834–10843. [[CrossRef](#)]
40. Selvaraj, M.; Jeon, S.H.; Han, J.; Sinha, P.K.; Lee, T.G. A novel route to produce 4-*t*-butyltoluene by *t*-butylation of toluene with *t*-butylalcohol over mesoporous Al-MCM-41 molecular sieves. *Appl. Catal. A Gen.* **2005**, *286*, 44–51. [[CrossRef](#)]
41. Perego, C.; Amarilli, S.; Carati, A.; Flego, C.; Pazzuconi, G.; Rizzo, C.; Bellussi, G. Mesoporous silica-aluminas as catalysts for the alkylation of aromatic hydrocarbons with olefins. *Microporous Mesoporous Mater.* **1999**, *27*, 345–354. [[CrossRef](#)]
42. Čejka, J.; Krejčí, A.; Žilková, N.; Dědeček, J.; Hanika, J. Alkylation and disproportionation of aromatic hydrocarbons over mesoporous molecular sieves. *Microporous Mesoporous Mater.* **2001**, *44–45*, 499–507. [[CrossRef](#)]
43. Selvaraj, M.; Sinha, P.K. Highly selective synthesis of *t*-butyl-*p*-cresol (TBC) by *t*-butylation of *p*-cresol with *t*-butyl alcohol over microporous and mesoporous catalysts. *J. Mol. Catal. A Chem.* **2007**, *264*, 44–49. [[CrossRef](#)]

44. Kamalakar, G.; Komura, K.; Sugi, Y. The Di-*t*-butylation of *p*-cresol with *t*-butanol in Supercritical CO₂ over Tungstophosphoric Acid Supported on Ordered Mesoporous Silica. *Catal. Lett.* **2006**, *108*, 31–35. [[CrossRef](#)]
45. Misono, M. Heterogeneous Catalysis by Heteropoly Compounds of Molybdenum and Tungsten. *Catal. Rev.* **1987**, *29*, 269–321. [[CrossRef](#)]
46. Molnár, Á.; Keresszegi, C.; Török, B. Heteropoly acids immobilized into a silica matrix: Characterization and catalytic applications. *Appl. Catal. A Gen.* **1999**, *189*, 217–224. [[CrossRef](#)]
47. Zhang, J.; Zhu, Z.; Li, C.; Wen, L.; Min, E. Characterization and kinetic investigation of tungstophosphoric supported on SiO₂ for alkylation of benzene with 1-dodecene to synthesize linear alkylbenzene. *J. Mol. Catal. A Chem.* **2003**, *198*, 359–367. [[CrossRef](#)]
48. Kaur, J.; Griffin, K.; Harrison, B.; Kozhevnikov, I.V. Friedel–Crafts Acylation Catalysed by Heteropoly Acids. *J. Catal.* **2002**, *208*, 448–455. [[CrossRef](#)]
49. Mizuno, N.; Misono, M. Heterogeneous Catalysis. *Chem. Rev.* **1998**, *98*, 199–218. [[CrossRef](#)]
50. Kozhevnikov, I.V. Catalysis by Heteropoly Acids and Multicomponent Polyoxometalates in Liquid-Phase Reactions. *Chem. Rev.* **1998**, *98*, 171–198. [[CrossRef](#)]
51. Mohana, R.K.; Gobetto, R.; Iannibello, A.; Zecchina, A. Solid state NMR and IR studies of phosphomolybdenum and phosphotungsten heteropoly acids supported on SiO₂, γ-Al₂O₃, and SiO₂—Al₂O₃. *J. Catal.* **1989**, *119*, 512–516. [[CrossRef](#)]
52. Kasztelari, S.; Moffat, J.B. The oxidation of methane on heteropolyoxometalates III. Effect of the addition of cesium on silica-supported 12-molybdophosphoric acid, molybdena, vanadia, and iron oxide. *J. Catal.* **1988**, *112*, 54–65. [[CrossRef](#)]
53. Kozhevnikov, I.V.; Sinnema, A.; Jansen, R.J.J.; Pamin, K.; Van Bekkum, H. New acid catalyst comprising heteropoly acid on a mesoporous molecular sieve MCM-41. *Catal. Lett.* **1994**, *30*, 241–252. [[CrossRef](#)]
54. Devassy, B.M.; Halligudi, S.B.; Hegde, S.G.; Halgeri, A.B.; Lefebvre, F. 12-Tungstophosphoric acid/zirconia—A highly active stable solid acid—Comparison with a tungstate zirconia catalyst. *Chem. Commun.* **2002**, *10*, 1074–1075. [[CrossRef](#)] [[PubMed](#)]
55. Bhatt, N.; Patel, A. Liquidphase *tert*-butylation of cresols catalysed by 12-tungstophosphoric acid and 12-tungstosilicic acid supported onto neutral alumina. *Catal. Lett.* **2007**, *113*, 99–103. [[CrossRef](#)]
56. Kumbar, S.M.; Shanbhag, G.V.; Lefebvre, F.; Halligudi, S.B. Heteropoly acid supported on titania as solid acid catalyst in alkylation of *p*-cresol with *tert*-butanol. *J. Mol. Catal. A Chem.* **2006**, *256*, 324–334. [[CrossRef](#)]
57. Kurhade, A.; Zhu, J.; Hu, Y.; Dalai, A.K. Surface Investigation of Tungstophosphoric Acid Supported on Ordered Mesoporous Aluminosilicates for Biodiesel Synthesis. *ACS Omega* **2018**, *3*, 14064–14075. [[CrossRef](#)]
58. Dias, A.S.; Pillinger, M.; Valente, A.A. Mesoporous silica-supported 12-tungstophosphoric acid catalysts for the liquid phase dehydration of d-xylose. *Microporous Mesoporous Mater.* **2006**, *94*, 214–225. [[CrossRef](#)]
59. Huang, J.; Fan, Y.; Zhang, G.; Ma, Y. Protective dissolution: Generating secondary pores in zeolite by mechanochemical reaction. *RSC Adv.* **2020**, *10*, 13583–13590. [[CrossRef](#)]
60. Aboul-Gheit, A.K.; Al-Hajjaji, M.A.; Summan, A.M. Differential scanning calorimetry probes acidity strength distribution in catalytic materials. *Thermochim. Acta* **1987**, *118*, 9–16. [[CrossRef](#)]
61. Aboul-Gheit, A.K. Desorption of presorbed ammonia, triethylamine and pyridine from the acid sites of mordenites via differential scanning calorimetry. *Thermochim. Acta* **1988**, *132*, 257. [[CrossRef](#)]
62. Kim, Y.S.; Wang, F.; Hickner, M.; Zawodzinski, T.A.; McGrath, J.E. Fabrication and characterization of heteropolyacid (H3PW12O40)/directly polymerized sulfonated poly (arylene ether sulfone) copolymer composite membranes for higher temperature fuel cell applications. *J. Membr. Sci.* **2003**, *212*, 263–282. [[CrossRef](#)]
63. Abedin, M.A.; Kanitkar, S.; Kumar, N.; Wang, Z.; Ding, K.; Hutchings, G.; Spivey, J.J. Probing the Surface Acidity of Supported Aluminum Bromide Catalysts. *Catalysts* **2020**, *10*, 869. [[CrossRef](#)]
64. Bachiller-Baeza, B.; Anderson, J.A. FTIR and reaction studies of the acylation of anisole with acetic anhydride over supported HPA catalysts. *J. Catal.* **2004**, *228*, 225–233. [[CrossRef](#)]
65. Asiedu, A.; Davis, R.; Kumar, S. Catalytic transfer hydrogenation and characterization of flash hydrolyzed microalgae into hydrocarbon fuels production (jet fuel). *Fuel* **2020**, *261*, 116440. [[CrossRef](#)]
66. Nie, P.; Liu, X.; Zhang, P.; Yuan, X.; Li, X.; Lin, S.; Yin, Z. Quaternary ammonium cellulose promoted synthesis of hollow nano-sized ZSM-5 zeolite as stable catalyst for benzene alkylation with ethanol. *J. Mater. Sci.* **2021**, *56*, 8461–8478. [[CrossRef](#)]
67. Yang, E.; Moon, D.J. CO₂ Reforming of Methane over Ni₀/La₂O₃ Catalyst Without Reduction Step: Effect of Calcination Atmosphere. *Top. Catal.* **2017**, *60*, 697–705. [[CrossRef](#)]
68. Yan, T.; Yang, L.; Dai, W.; Wang, C.; Wu, G.; Guan, N.; Hunger, M.; Li, L. On the deactivation mechanism of zeolite catalyst in ethanol to butadiene conversion. *J. Catal.* **2018**, *367*, 7–15. [[CrossRef](#)]
69. Alamdari, R.F.; Hosseinabadi, Z.; Khouzani, M.F. Synthesis, characterization and investigation of catalytic activity of Cu_{1-x}Co_x Fe₂O₄ nanocatalysts in *t*-butylation of *p*-cresol. *J. Chem. Sci.* **2012**, *124*, 827–834. [[CrossRef](#)]
70. Roselin, L.S.; Selvin, R.; Aneesh, P.; Bououdina, M.; Krishnaswamy, S. Highly Active and Reusable Catalyst for Fries Rearrangement of Phenyl Acetate. *Kinet. Catal.* **2011**, *52*, 823–827. [[CrossRef](#)]

71. Chen, D.; Rebo, H.P.; Moljord, K.; Holmen, A. Influence of Coke Deposition on Selectivity in Zeolite Catalysis. *Ind. Eng. Chem. Res.* **1997**, *36*, 3473–3479. [[CrossRef](#)]
72. Subramanian, S.; Mitra, A.; Satyanarayana, C.V.V.; Chakrabarty, D.K. Para-selective butylation of phenol over silicoaluminophosphate molecular sieve SAPO-11 catalyst. *Appl. Catal. A Gen.* **1997**, *159*, 229–240. [[CrossRef](#)]

Disclaimer/Publisher’s Note: The statements, opinions and data contained in all publications are solely those of the individual author(s) and contributor(s) and not of MDPI and/or the editor(s). MDPI and/or the editor(s) disclaim responsibility for any injury to people or property resulting from any ideas, methods, instructions or products referred to in the content.